analytical chemistry

pubs.acs.org/ac Article

Therapeutic Monoclonal Antibody—Antidrug Antibody Affinity Constant Determination Using Capillary Electrophoresis–Tandem Mass Spectrometry

Tessa Reinert,* Pascal Houzé, Nathalie Mignet, Aynur Naghizade, Lola Alez-Martin, Oscar Hernandez-Alba, Armand Leclerc, Sarah Cianferani, Rabah Gahoual, and Yannis-Nicolas Francois

Cite This: https://doi.org/10.1021/acs.analchem.4c02932 Read Online

ACCESS | Metrics & More | Article Recommendations | Supporting Information

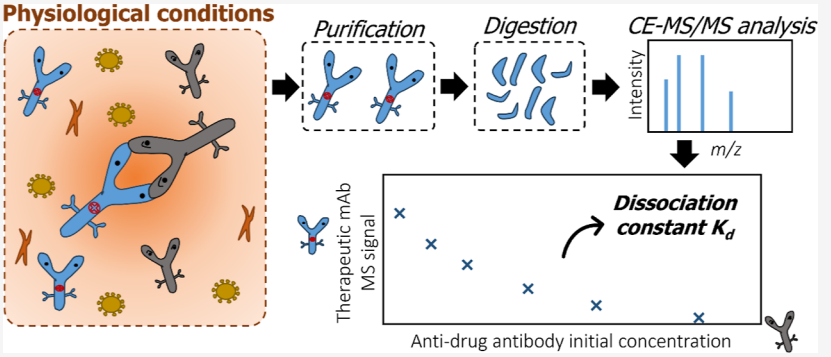

ABSTRACT: Monoclonal antibody (mAbs) therapeutics cannot evade the occurrence of adverse effects. Thus, mAbs are commonly triggering immune responses corresponding to the expression of antidrug antibodies. Antidrug antibodies can neutralize mAbs, leading to their inhibition and hasten clearance, which dramatically hampers their therapeutic effects. Therefore, studies concerning the affinity between a mAbs and the corresponding antidrug antibody are demonstrating a growing interest to further understand the outcome of biotherapeutics after administration. We describe a novel analytical approach for the determination of the dissociation constant (K_d) between a mAb and an antidrug antibody using capillary electrophoresis coupled to mass spectrometry (CE-MS/MS). The CE-MS/MS method employs a competitive assay, followed by the quantification of the residual amount of the active mAbs. The methodology allowed for the measurement of K_d using serum samples without the implementation of immobilization to achieve protein–protein interaction. This characteristic enabled us to generate the interaction in conditions reflecting the physiological environment. A mathematical treatment was developed to calculate K_d from MS/MS data, taking into account the stoichiometry of the mAbs/antidrug antibody complex and the bivalent properties of the two immunoglobulins. Prior to CE-MS/MS analysis, the interaction of the two proteins was studied by using mass photometry (MP) to determine equilibrium conditions and complexation stoichiometry. CE-MS/MS was used to investigate the interaction between infliximab and a neutralizing anti-infliximab antibody. Results allowed to measure a K_d of 14.4 ± 2.9 nM. MS instrumentation sensitivity and specificity showed to be relevant to achieve accurate and robust K_d measurements for strong interactions in the nanomolar range.

Monoclonal antibodies (mAbs) and their related formats, such as bispecific antibodies, fusion proteins, or antibody-drug conjugates, currently represent a significant proportion of biopharmaceutical products. Their development and successful therapeutic applications have undoubtedly contributed to the advent of this pharmaceutical field, with 175 approved products, including 19 in 2022, and more than 140 reported in clinical trials.[1] Rationally, therapeutic proteins, such as mAbs, are expected to have lower toxicity compared with cytotoxic molecules. However, mAbs are particularly prone to induce immunogenic reactions.[2] For instance, the patient's immune system may express neutralizing antidrug antibodies (NADAs). NADAs can target the antigen binding fragments (F_{ab}), resulting in the inhibition of the therapeutic mAb from binding its corresponding antigen normally. Neutralization of therapeutic mAbs by NADAs can compromise their efficacy and hasten their clearance, which in most adverse cases could lead to complete inactivation.[3] The expression of NADAs after injection of mAbs remains challenging in several aspects.

Received: June 7, 2024
Revised: November 15, 2024
Accepted: November 19, 2024

Indeed, this type of immune response is not systematic among the treated populations without any clear attributions so far regarding the causalities of this phenomenon. In addition, their episodic presence complicates the therapeutic management of patients and urges the implementation of a dedicated follow-up.

A variety of approaches have been used to determine antibody affinities, including surface plasmon resonance (SPR)[4] and indirect and competitive immunoassays.[5] The latter aims to determine the apparent affinities of a system by assessing the concentration of unbound active antibodies in a solution. This is done after preincubation of the antibody solution with predetermined molar concentrations of the corresponding antigen and can be performed in the matrix. Bobrovnik et al. and Stevens et al. introduced a novel approach that is based on competitive enzyme-linked immunosorbent assays (ELISAs) and facilitated the determination of apparent antigen-mAb affinity derived from the law of mass action.[6−8] The strategy was then applied to determine mAb affinities with receptors or antigens.[9,10]

Although the equilibrium state can be achieved in the matrix system, ELISA technologies are known to be affected by serum interference.[11,12] Similarly, the immobilization of mAbs on the surface of ELISA wells required to perform the analysis can lead to epitope alteration or an unfavorable presentation. In addition, the multiple wash steps can dissociate low affinity interactions, resulting in negative results and interfering with the affinity measurement.[13,14] All of these issues can alter the quantification of unbound active mAbs by ELISA and thus affect the determination of affinity. The use of SPR for affinity measurement is quite robust;[15] however, it also requires the immobilization of mAbs on SPR sensor. In addition, the aforementioned approaches were originally established for bivalent antibodies binding to monovalent antigens and therefore need to be adapted for the mAb-to-mAb affinity assessment.

The current study overcomes these issues to determine the dissociation constant between two antibodies in the serum. After preincubation of the mAbs solution, the absolute quantification of unbound active antibodies is performed using capillary electrophoresis hyphenated to tandem mass spectrometry (CE-MS/MS) analysis,[16] allowing the determination of the experimental dissociation constant K_d between the therapeutic antibody infliximab (IFX) and a neutralizing antidrug antibody, referred to as neutralizing antibody-to-infliximab (NATI). IFX is a chimeric mAb targeting tumor necrosis factor α (TNF-α) to inhibit the pro-inflammatory activity of TNF-α, observed in inflammatory bowel diseases such as Crohn's disease. Because of its use in the treatment of chronic disease, IFX must be injected regularly to maintain an optimal suppression of symptoms as long as the symptoms last. However, recent studies highlighted that 38% of patients expressed NATIs after 12 months of treatment.[17]

Prior to CE-MS/MS experiments, MP analysis was performed on samples consisting of a mixture of stable-isotope-labeled infliximab (SIL-IFX) and NATI to investigate the stoichiometry and kinetics of IFX/NATI complexation. Then, CE-MS/MS analysis allowed accurate quantification of the fraction of active IFX remaining after equilibrium and non-neutralized by NATI. This concentration was determined using an internal standard consisting of an isotopically labeled adalimumab (SIL-ADM), also initially introduced into the model serum. To be compatible with CE-MS/MS analysis, active IFX and SIL-ADM were extracted from serum samples using an affinity purification process developed in-house based on magnetic beads functionalized with TNF-α. Subsequently, the purified mAbs were submitted to proteolytic digestion, and the resulting peptide mixture obtained was characterized by CE-MS/MS. Finally, the IFX/NATI dissociation constant K_d was deduced from the absolute quantification of active IFX and was found in the nanomolar range. Several developments regarding the methodology to calculate the K_d value from CE-MS/MS data were also introduced in this study, especially in order to consider the complexity due to the bivalence of IFX and NATI, respectively.

MATERIALS AND METHODS

Chemicals. The experiments were performed with isotopically labeled analogues of infliximab and adalimumab, which are expected to have reactivities and affinities identical to those of the unlabeled mAbs. Stable isotopes labeled infliximab (SIL-IFX) and adalimumab (SIL-ADM), labeled on arginine ($^{13}C_6$; $^{15}N_4$) and lysine ($^{13}C_6$; $^{15}N_2$) residues, were supplied by Sigma-Aldrich (Saint-Quentin Fallavier, France). A full-length human antiidiotypic antibody against IFX (clone AbD17841_hIgG1) used as a model NATI was obtained from Bio-Rad Laboratories (Marnes-La-Coquette, France). Streptavidin M-280 Dynabeads and biotinylated TNF-α were obtained from Fisher Scientific Invitrogen (Illkirch, France). Sequencing-grade modified trypsin was purchased from Promega Corp. (Madison, WI, USA).

Preparation of IFX Quantification Calibration Samples. Standard solutions used to construct IFX calibration curves were prepared from a blank serum, obtained from the French Institute of Blood (Paris, France), spiked with increasing IFX concentrations ranging from 1 to 25 $\mu g \cdot mL^{-1}$ and ADM at a fixed concentration of 10 $\mu g \cdot mL^{-1}$.

K_d Determination Sample Elaboration. Model serum samples used for K_d determination were prepared from 100 μL of blank serum spiked with a fixed concentration of ADM and IFX (10 $\mu g \cdot mL^{-1}$ each) and increasing concentrations of NATI ranging from 1 to 30 $\mu g \cdot mL^{-1}$. Afterward, samples were incubated for 1h at 20 °C prior to further treatment.

CE-MS/MS Sample Preparation. The preparation of serum samples was derived from the protocol recently published by our group.[18] Briefly, ferromagnetic beads (Dynabeads) and biotinylated TNF-α were mixed and incubated for 1 h at 20 °C. The serum solution was then added to the functionalized beads and incubated for 1h at RT to allow the TNF-α inhibitors IFX and ADM to bind to the beads. After elimination of the serum, acidic dissociation was performed by adding a MeOH/H_2O/FA (48.5/48.5/3; v/v/v) solution to elute mAbs from the surface of the beads. The supernatant was dried, and consequently, 70 μL of ammonium bicarbonate buffer (50 mM, pH 8) was used to reconstitute the sample prior to the denaturation-reduction-alkylation-digestion workflow, which is commonly used for the bottom-up strategy of mAbs.[19] Finally, the peptide digest was dried and reconstituted in 5 μL of ammonium acetate, 100 mM, pH 4.

MP Analysis. MP experiments were carried out using a TWO^{MP} mass photometer (Refeyn Ltd., Oxford, UK) at room temperature. Microscope coverslips (24 × 50 mm, Fisher Scientific and 24 × 24 mm, Globe Scientific) were prepared by sequential rinsing with isopropanol and H_2O, followed by drying under ultrapure nitrogen. PBS solutions containing NATI (3 $\mu g \cdot mL^{-1}$) and IFX (3 $\mu g \cdot mL^{-1}$) were incubated for

https://doi.org/10.1021/acs.analchem.4c02932
Anal. Chem. XXXX, XXX, XXX−XXX

Table 1. Ions of Surrogate's Peptides for SIL-IFX and SIL-ADM

peptide sequence	name	analyte	role	precursor (m/z)	product ions (m/z)	
					y9-967.54	**y6**-654.34
DILLTQSPAILSVSPGE**R*** (^{13}C,^{15}N)	IFX*$_{LC01}$	SIL-IFX	Quantifier	953.53	y8-854.34	**y5**-555.27
					y7-741.37	
					y8-909.45	**y5**-498.27
EVQLVESGGGLVQPGG**R*** (^{13}C,^{15}N)	ADM*$_{HC01}$	SIL-ADM	Internal standard	817.94	y7-746.39	**y4**-441.25
					y6-645.34	

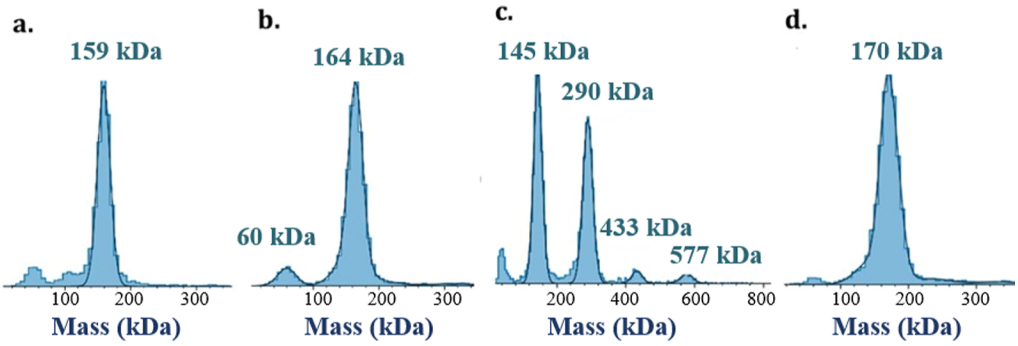

Figure 1. MP spectra for (a) SIL-IFX at 3 μg·mL^{-1}, (b) NATI antibody at 3 μg·mL^{-1}, (c) SIL-IFX and NATI mixture at 3 μg·mL^{-1} and (d) incubation of NATI and SIL-ADM both at 3 μg·mL^{-1}.

different times (1−60 min) before being loaded into the six-well reusable silicone gaskets (CultureWellTM, 50−3 mm DIA x 1 mm Depth, 3−10 μL, Grace Bio-Laboratories, Inc., Oregon, USA) assembled on the cover slide. Images were processed using DiscoverMP software (Refeyn Ltd., Oxford, UK). The relative intensities of the identified species were calculated with the individual number of counts obtained for each population upon Gaussian fitting.

Capillary Electrophoresis-Tandem Mass Spectrometry Analysis. CZE-ESI-MS/MS experiments were performed using a CESI8000 capillary electrophoresis system (Sciex separations, Darmstadt, Germany) coupled to a Sciex 5600 TTOF mass spectrometer (Darmstadt, Germany) with a sheathless interface. The separation capillary, filled with the background electrolyte (BGE, 10% acetic acid), was made of bare fused silica (total length 100 cm; 30 μm i.d.). For each analysis, a volume of 68 nL was hydrodynamically injected (5 psi, 100 s), and a voltage of +23 kV was applied for the separation. The ESI voltage was −1.5 kV; the source heating temperature was 100 °C; and the curtain gas was set to 2. Experiments were performed in Top20 information-dependent acquisition (IDA, Sciex) with a total duty cycle of 1.9 s during 60 min of analysis.

Active IFX Quantification. The quantification of active IFX was based on the area of the peak corresponding to the proteospecific peptide IFX*$_{LC01}$ (Table 1). In order to provide robust IFX absolute quantification, ADM was used as an internal standard and measured by the intermediate of the peptide ADM*$_{HC01}$ (Table 1). MS and MS/MS spectra were studied to ensure unambiguous identification of the two compounds. The IFX peptide IFX*$_{LC01}$ is located on the variable part of infliximab, and its specificity was verified by a blast search against a human proteome database. Further details are discussed in the Supporting Information.

RESULTS AND DISCUSSION

IFX/NATI Complexation MP Study. A multistep approach was used to characterize the interaction between IFX and NATI. First, MP analysis was performed to provide insights on the interaction between the different mAbs included in the study. MP is a relatively new technique based on the interferometric scattering microscopy principle (iSCAT) as a means for detecting and measuring the mass of biomolecules and their complexes.[20,21] Briefly, the molecular entities in solution bind the microscope cover glass surface in a nonspecific manner. This interaction alters the local reflectivity, generating a contrast signal as a result of interference between the scattered and reflected lights. The magnitude of the interference (or contrast) can be correlated to the mass of the entity of interest upon calibration with biomolecules of known masses.[22] Therefore, MP is a label-free method that detects biomolecules and their interactions in solution at the single molecule level. The versatility and sensitivity of this measurement have spurred the use of MP to characterize a wide range of biological samples, such as adeno associated virus,[23] membrane proteins,[24,25] monoclonal antibodies,[26] ribosomal particles, and ribonucleotides.[27,28]

In our study, MP analysis was performed on samples containing solely IFX or NATI diluted in PBS. As emphasized in Figure 1a., the MP spectrum in the case of IFX alone showed a single peak presenting an average molecular mass of 159 kDa (standard deviation σ: 13 kDa). Similarly, the analysis of NATI demonstrated a single peak presenting an average mass of 164 kDa (σ, 20 kDa, Figure 1b.). Therefore, the MP experiments showed that both spectra were governed by the monomeric structure of the mAbs, with no experimental evidence supporting the presence of higher-molecular-weight species (HMWS). Consequently, equimolar mixtures of IFX and NATI in PBS were incubated for 1 h at 20 °C and analyzed by MP. As shown in Figure 1c., the mass of the most intense species was calculated at 145 kDa (σ: 13 kDa), corresponding to free IFX and NATI mAbs. Several signals were detected beyond 200 kDa as a result of the interaction between both mAbs. The mass of the most intense complex signal was 290 kDa (σ: 14 kDa), which was attributed to a 1:1 IFX−NATI complex. In addition, MP spectra exhibited a weak

https://doi.org/10.1021/acs.analchem.4c02932
Anal. Chem. XXXX, XXX, XXX−XXX

signal at mass 433 kDa (σ: 15 kDa), which could be attributed to the formation of complexes presenting 1:2 and/or 2:1 stoichiometries. Finally, the MP data showed the identification of HMWS with a mass of 577 kDa (σ: 18 kDa), potentially corresponding to a 2:2 stoichiometry between both mAbs.

To demonstrate the specificity of NATI to neutralize IFX, a mixture of adalimumab (ADM) and NATI was analyzed under conditions similar to those for a negative control. ADM is another type of mAb targeting TNF-α. After incubation, MP data revealed a single signal at 170 kDa corresponding to the mixture of ADM and NATI, suggesting that the two mAbs do not interact to form HMWS (Figure 1d.), thus corroborating the specificity of NATI to bind IFX F_{ab}. Therefore, the MP data revealed a predominant 1:1 stoichiometry in the interaction between IFX and NATI. Drawing from this finding, a critical aspect required further exploration due to the bivalence inherent in both proteins owing to their IgG1 nature. Hence, in the presence of NATI, IFX can exist in an unliganded state, a singly liganded state, or a doubly liganded form, as illustrated in Figure 2. In its singly liganded configuration, IFX can bind to a NATI on one F_{ab} and remain active, as it can still bind its other arm to TNF-α.

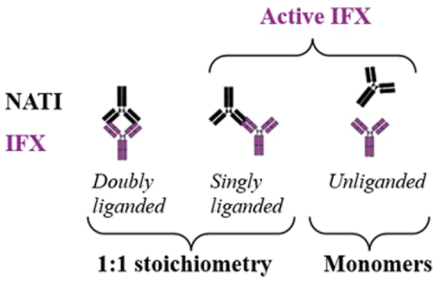

Figure 2. Schematic representation of the different forms of infliximab/NATI interaction for a 1:1 stoichiometry. Noncomplexed infliximab or experiencing single F_{ab} complexation remains active.

Following the IFX/NATI stoichiometry determination, a kinetic study of the neutralization was performed using MP analysis. Samples consisting of NATI and IFX in PBS were analyzed at different incubation times. As emphasized in Figure 3a, the relative proportion of the 4 peaks observed for the MP data (Figure 1c) showed a rapid formation of the 1:1 complex, correlated with a decrease of the peak corresponding to IFX and NATI monomers. After 5 min, the relative distribution of monomers and 1:1 complex remained stable, indicating that an equilibrium was reached. The MP data exhibited 1:2 and 2:2 stoichiometries that were systematically present below 4% regardless of the incubation time. Based on these results and assuming that IFX-NATI interaction stoichiometry is identical regardless of the sample composition (PBS or serum), only the 1:1 complex was considered to be formed in the serum sample. Consequently, the proportion of each species at an equilibrium was performed by varying the initial concentration of NATI to evaluate the relative proportion of the observed species. MP data demonstrated essentially the formation of a 1:1 IFX/NATI complex, even when NATI was present in large excess compared to IFX (Figure 3b).

This observation was attributed to the specific nature of the interaction between the IFX F_{ab} regions and NATI. However, it was observed that higher proportions of NATI (beyond the 1.7 ratio, Figure 3b) led to increased relative intensities of the free mAb signal. This observation is the direct consequence of the low MP mass resolution, which impairs the differentiation between the two NATI and IFX mAbs with close molecular masses. The relative intensities of 1:2 and 2:2 stoichiometry complexes remained stable and below 10% (6.0 ± 2.3% and 6.8 ± 2.9%, respectively) with increasing NATI concentrations.

Red dots: free mAbs (signal at 145 kDa), green dots: 1:1 stoichiometry (signal at 290 kDa), blue dots: 1:2 or 2:1 stoichiometry (signal at 433 kDa), and black dots: 2:2 stoichiometry (signal at 577 kDa).

CE-MS/MS Analysis for IFX/NATI Interaction K_d Determination. A dedicated workflow was developed to experimentally measure the IFX/NATI K_d constant, as represented in Figure 4. The CE-MS/MS analytical strategy was derived from a competitive binding assay. Model serum samples were spiked with known amounts of IFX and NATI and left to generate IFX-NATI complexation in a state as close as possible to in vivo conditions. The fraction of active IFX (i) that did not form complexes with NATI was then specifically extracted and quantified using CE-MS/MS. To ensure accurate and precise quantification of this remaining active IFX, an internal standard consisting of stable-isotope-labeled adalimumab (ADM) was added to serum samples. ADM accounted for any bias originating from sample preparation or analysis, as it was not affected by NATI neutralization (Figure 1d). The active fractions of IFX and ADM were simultaneously extracted by affinity purification using magnetic beads with immobilized TNF-α.[29] The two extracted mAbs were then digested and analyzed using CE-MS/MS conditions recently developed by our group.[18] Finally, the plot of CE-MS/MS

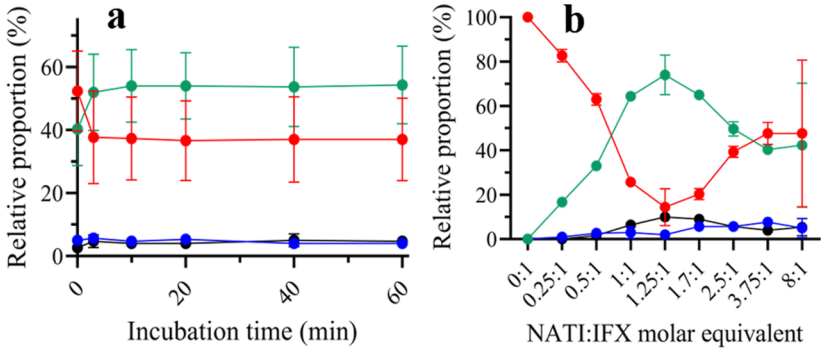

Figure 3. (a) Kinetic study of SIL-IFX/NATI complexation using MP in PBS. SIL-IFX and NATI concentrations were fixed at 3 $\mu g \cdot mL^{-1}$. (b) Evolution of species relative proportion depending on the NATI initial concentration for fixed SIL-IFX at 3 $\mu g \cdot mL^{-1}$ (n = 3, error bars represent the standard deviation).

https://doi.org/10.1021/acs.analchem.4c02932
Anal. Chem. XXXX, XXX, XXX−XXX

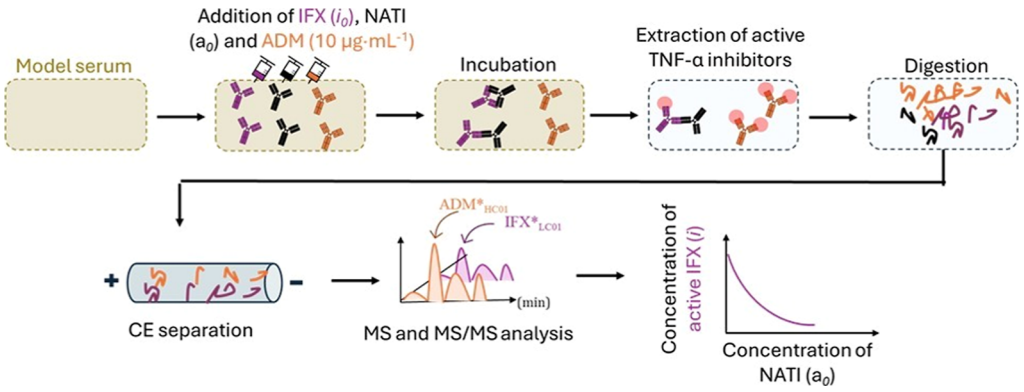

Figure 4. Workflow designed for the K_d determination of infliximab/NATI complex using CE-MS/MS analysis. Model serum samples were prepared using IFX and ADM spiked in similar concentrations (10 μg·L^{-1}) and different concentrations of NATI (0−30 μg·L^{-1}).

absolute quantification of the active fraction of IFX (i) as a function of spiked NATI concentration was used to accurately assess the dissociation constant (K_d) of the infliximab/NATI interaction (Figure 4).

Quantification of Active IFX. Prior to the determination of the K_d constant between IFX and NATI, the characteristics of IFX quantification using CE-MS/MS and ADM as an internal standard were first evaluated without the presence of NATI. Regarding selectivity, the analysis of serum samples spiked only with IFX and ADM showed that the selected two surrogate peptides (Table 1) exhibited significantly different mobilities, leading to their consistent separation in CZE (Figure S1a., Supporting Information). In addition, no interferences were observed in the extracted ion electropherograms of the two peptides (Figure S1b, Supporting Information). Consequently, the linearity between the ratios (r) of the surrogate peptides measured by CE-MS/MS as a function of the concentration of active SIL-IFX was investigated. Good repeatability and linearity were achieved for concentrations ranging from 1 to 25 μg·mL^{-1} (Figure 5). In

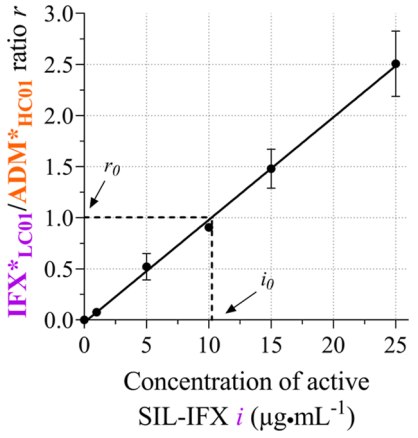

Figure 5. Evolution of IFX*$_{LC01}$/ADM*$_{HC01}$ peptide ratio with the concentration of IFX (0−25 μg·mL^{-1}). ADM concentration was fixed at 10 μg·mL^{-1} (n = 3). Linear regression y = 0.10 x−0.02 (r^2 = 0.982).

the case of serum spiked with IFX and ADM at an equivalent concentration of 10 μg·mL^{-1} (i_0), the peptide ratio was defined as r_0 = 1, as emphasized in Figure 5. Therefore, the CE-MS/MS data demonstrated that quantification of active IFX was possible over the concentration range considered. Therefore, the experiments suggested that by introducing IFX and ADM at equivalent concentrations into a serum sample potentially containing NATI, the evolution of the peptide ratios can be used to determine the concentration of active IFX (i) by the intermediate of this linear relationship (Figure 5).

Interaction between IFX and NATI Paratopes. To measure the dissociation constant of the IFX/NATI complex further experimentally, as described in Figure 4, a series of serum samples were prepared incorporating IFX and ADM systematically at 10 μg·mL^{-1} (i_0) with different concentrations of NATI (a_0). The serum samples were then analyzed using the CE-MS/MS analytical strategy developed in order to determine the ratio r between the surrogate peptides corresponding to IFX and ADM, respectively (Table 1). As previously determined, the value of r denotes the fraction of active IFX compared with the internal standard. Figure 6

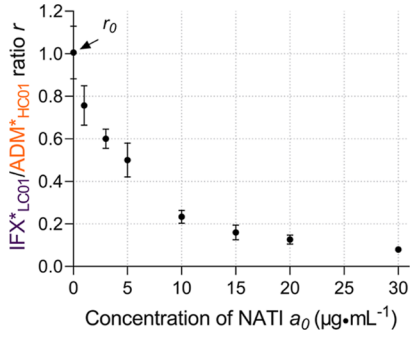

Figure 6. Ratio between IFX/ADM CE-MS/MS signals as a function of the initial concentration of neutralizing-antibodies-to-infliximab (NATI, a_0) added to serums. Error bars represent the standard deviation among the triplicates.

shows the ratio depending on the initial concentration of NATI. CE-MS/MS results demonstrated a progressive decline as the concentration of NATI increased. This phenomenon indicated the neutralizing effect of NATI, which resulted in the inhibition of IFX extraction during the purification process. This indicates the hampered biological activity of IFX.

The results presented in Figure 6 highlight crucial information about the IFX/NATI complexation. At an equimolar concentration (i_0 = a_0 = 10 μg·mL^{-1}), it appears that approximately 80% of the IFX antibodies were completely neutralized by the NATI (both paratopes bound) and were therefore not extracted by TNF-α. This could suggest that

https://doi.org/10.1021/acs.analchem.4c02932
Anal. Chem. XXXX, XXX, XXX−XXX

under native conditions, most NATI/infliximab interactions occur in a doubly liganded form (Figure 2).

Due to their IgG nature, both IFX and NATI are bivalent proteins. Thus, IFX may potentially be neutralized on the two F_{ab} arms. Similarly, NATI can be involved in the partial neutralization of two independent IFX molecules (Figure 2). As a consequence, the methodology used to calculate K_d values based on CE-MS/MS data was adapted to account for double bivalence. Therefore, to address this complexity, the two paratopes were considered independently for IFX and NATI, respectively. Table 2 presents the reaction table corresponding to the neutralization of IFX paratopes by NATI paratopes when IFX and NATI are introduced into the serum sample.

Table 2. Complexation Reaction of IFX and NATI Paratopes When Introduced in a Solution[a]

state	paratope (IFX) +	paratope (NATI) ↔	liganded paratopes
initial	$2i_0$	$2a_0$	0
equilibrium	$2i_0 - x$	$2a_0 - x$	x

[a]Term x defines the concentration of IFX/NATI paratopes complexes formed at an equilibrium. a_0 is the initial concentration of NATI ($\mu g \cdot mL^{-1}$), i_0 is the initial concentration of IFX ($\mu g \cdot mL^{-1}$), and x is the concentration of liganded paratopes ($\mu g \cdot mL^{-1}$).

Based on Table 2, the probability for a single IFX paratope to be neutralized at an equilibrium can be expressed using eq 1, as described previously for an antibody−antigen system[8]

$$p = \frac{x}{2i_0} \tag{1}$$

The inactivation of IFX resulted from the simultaneous neutralization of its two paratopes at an equilibrium (Figure 2). The probability of such an event could be expressed by the factor p^2. Therefore, the probability for IFX to remain potentially active after an equilibrium, due to having only 0 or 1 paratope neutralized, is expressed by the intermediate of eq 2

$$\frac{i}{i_0} = 1 - \left(\frac{x}{2i_0}\right)^2 \tag{2}$$

The analysis performed using the CE-MS/MS method enabled us to quantify the fraction of active IFX (i/i_0). Indeed, inactive IFX evaded the affinity purification step, resulting in the quantification of the active IFX alone. Using this characteristic and the proportional relationship between the fraction of active IFX (i) and the IFX/ADM peptide ratio (r) determined previously (Figures 5 and 6); the concentration of totally bound IFX/NATI paratopes is obtained (further details are discussed in the Supporting Information)

$$x = 2i_0\sqrt{1 - r} \tag{3}$$

Based on the law of mass action, the dissociation constant of the IFX/NATI paratope interaction is defined as

$$K_d = \frac{(2a_0 - x)(2i_0 - x)}{x} \tag{4}$$

Equation 3 is further transposed into eq 4, resulting in the establishment of the following expression

$$\frac{a_0 - i_0\sqrt{1 - r}}{K_d} = \frac{\sqrt{1 - r}}{2 \times (1 - \sqrt{1 - r})} \tag{5}$$

It was assumed that the extraction of the active IFX from the serum using TNF-α functionalized beads does not readjust the equilibrium of IFX/NATI neutralization. Equilibrium readjustment was found to be negligible in a previous study for another antigen/antibody complex after extraction in ELISA plates.[30] This property was explained by the nanomolar affinities involved in the interactions between IFX and NATI or TNF-α. Therefore, such important affinities favored the formation of complex compared with complex disassembly, considering the concentration of IFX and NATI present in serum samples.

Consequently, the right-hand side of eq 5 is plot as a function of $(a_0 - i_0\sqrt{1 - r})$ in Figure 7, using data obtained

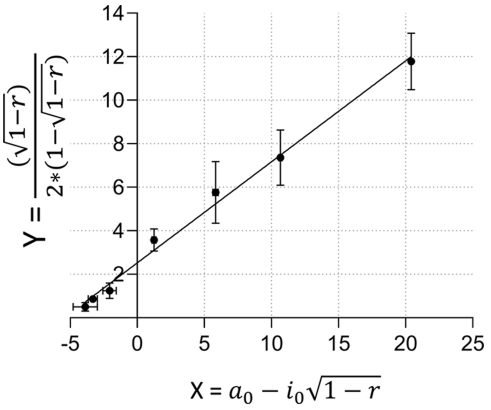

Figure 7. Plot of $(\sqrt{1 - r})/(2 \times (1 - \sqrt{1 - r}))$ as a function of $(a_0 - i_0\sqrt{1 - r})$ for initial concentration of NATI (a_0) ranging from 0 to 30 $\mu g \cdot mL^{-1}$. Linear regression $y = 0.46x - 2.5$ ($r^2 = 0.958$). Error bars represent the standard deviation among triplicates.

from CE-MS/MS experiments. The dissociation constant K_d between IFX and NATI, corresponding to the inverse of the slope, was found to be 14.4 ± 2.9 nM. The error was calculated as the 95% confidence interval of the slope. The linear regression and experimental data demonstrated a good correlation, indicating that the experimentally determined K_d constant using CE-MS/MS data was stable for the concentration range of NATI considered. The results showed that the K_d values determined experimentally were in a similar range compared to other isotypes of anti-IFX antibodies described in the literature.[31] As expected, dissociation constants measured in the nanomolar range demonstrated the important affinity regulating the IFX/NATI interaction. Therefore, the CE-MS/MS analytical strategy demonstrated the possibility of determining extremely low dissociation constants. In addition, the experiments were performed in a native environment composed of human serum, which allowed the experiments to be positioned closer to in vivo conditions. ELISA assays and SPR, conventionally used to characterize protein−protein dissociation constants, rely on the immobilization of mAbs on different types of surfaces.[4,32] However, these methodologies may hinder the interaction if the mAbs are not properly oriented, exposing their variable domains, which could lead to a systematic bias in the K_d determination.

It is important to note, regarding the CE-MS/MS analytical strategy, that the calculated K_d reflects the global affinity of all IFX paratopes existing in the mixed valences of the F_{ab} region.

https://doi.org/10.1021/acs.analchem.4c02932
Anal. Chem. XXXX, XXX, XXX−XXX

The intrinsic affinity of a local IFX(paratope)/NATI-(paratope) interaction may differ depending on whether the two proteins are singly liganded or doubly liganded (Figure 2).[33] Therefore, the intrinsic affinity of a single IFX paratope may vary depending on whether the second IFX F_{ab} is already involved in an interaction with a NATI paratope.

To conclude, the analytical methodology developed using affinity purification followed by CE-MS/MS analysis allowed the dissociation constant between IFX and NATI paratopes to be measured in a reliable manner, while minimizing artifacts and preserving the native state of the two proteins. The method conditions were designed in order to be compatible with subsequent CE-MS/MS analysis. Thus, for the first time, this analytical technique could be applied to a peptide-centric approach for the measurement of protein−protein dissociation constants. Results showed the capacity of the developed strategy to measure the concentration of active IFX in a biological sample in addition to distinguishing faint changes concerning the levels of active mAbs. This property allowed for the consistent calculation of the dissociation constant corresponding to the neutralization of IFX by NATI. The methodology provided valuable insights into the IFX/NATI interaction and demonstrated the possibility of maintaining the natural diffusion of both antibodies within the biological matrix, without any labeling or surface functionalization during the complexation. The incorporation of the ADM internal standard was particularly important, as it allowed us to account for losses and biases potentially originating from sample preparation, thereby improving the reproducibility and robustness of the method. Also, it allowed the estimation of the amount of neutralized IFX, and thus the value of the dissociation constant, without any structural information regarding the NATI antibody, such as the amino acid sequence or the molecular mass of the protein. Thus, the CE-MS/MS analytical approach was not restricted to the analysis of a single isotype of NATI but can be used to characterize any isotype responsible for the neutralization of IFX. Consequently, it is possible to use the analytical strategy based on CE-MS/MS for the detection of the immune response in samples originating from patients regardless of the isotype expressed by their immune system.

CONCLUSIONS

An integrated methodology was developed to characterize the interaction between therapeutic mAbs IFX and a neutralizing antibody-to-infliximab NATI, commonly expressed due to immunogenic reactions in patients. MP analysis was performed on IFX/NATI mixtures in order to determine the stoichiometry of the complex formed consequently to neutralization. In addition, the MP results allowed us to demonstrate the specificity and investigate the kinetics of NATI neutralization. Consequently, a novel analytical strategy based on a label-free and immobilization-free method was designed and implemented to experimentally measure the dissociation constant between IFX and NATI, directly performed in biological matrices. The approach utilized affinity purification prior to CE-MS/MS analysis using an internal standard in order to eliminate any potential bias due to the sample treatment analysis. CE-MS/MS was performed to provide an accurate determination of active IFX quantities in the presence of NATI. A robust mathematical model, compatible with CE-MS/MS data and taking into account the bivalent characteristics of both IFX and NATI, allowed experimental measurement of the apparent dissociation constant of IFX/NATI complexation. As a result, the dissociation constant was calculated from the intermediate of concentrations of active IFX in model serums in the presence of NATI. To our knowledge, CE-MS/MS has never been used to determine the dissociation constant between therapeutic mAbs and their corresponding antidrug antibodies. The application of the CE-MS/MS analytical strategy allowed us to measure an IFX/NATI dissociation constant of 14.4 ± 2.9 nM showing relevant affinities for this type of high-binding interaction.

The CE-MS/MS analytical strategy demonstrated the ability to study the IFX/NATI affinity under conditions that are particularly close to in vivo conditions. The results showed that the measurement of the quantity of active IFX using an independent internal standard provided the ability to measure the dissociation constant without any structural information regarding NATI. Therefore, the CE-MS/MS analytical strategy could be applied to measure the dissociation constant of other NATI isotypes using the same methodology and method conditions. Also, CE-MS/MS enabled to target neutralizing antibodies in a specific manner compared to commercial ELISA assays that may detect anti-IFX antibodies regardless of their neutralizing capacities. As a consequence, CE-MS/MS analysis could be used for the analysis of patient serums in order to identify unambiguously the occurrence of an immune response in the form of NATI expression. In addition, further developments of the CE-MS/MS analytical strategy could be implemented to provide simultaneous absolute quantification of IFX and NATI, for instance to monitor the occurrence of immune responses and estimate the level of immune response against the administered therapeutic mAbs.

ASSOCIATED CONTENT

Supporting Information

The Supporting Information is available free of charge at https://pubs.acs.org/doi/10.1021/acs.analchem.4c02932.

MS data monitoring of the two selected surrogate peptides and calculation for affinity assessment (PDF)

AUTHOR INFORMATION

Corresponding Author

Tessa Reinert − *Laboratoire de Spectrométrie de Masse des Interactions et des Systèmes (LSMIS), Université de Strasbourg, CNRS UMR7140, CMC, Strasbourg 67081, France; Université Paris Cité CNRS, Inserm, Unité de Technologies Chimiques et Biologiques pour la Santé (UTCBS), Faculté de Sciences Pharmaceutiques et Biologiques, Paris 75270, France;* orcid.org/0009-0005-7434-8450; Email: tessa.reinert@univ-lyon1.fr

Authors

Pascal Houzé − *Université Paris Cité CNRS, Inserm, Unité de Technologies Chimiques et Biologiques pour la Santé (UTCBS), Faculté de Sciences Pharmaceutiques et Biologiques, Paris 75270, France; Laboratoire de Toxicologie Biologique, Hôpital Lariboisière, Assistance Publique − Hôpitaux de Paris (AP-HP), Paris 75010, France*

Nathalie Mignet − *Université Paris Cité CNRS, Inserm, Unité de Technologies Chimiques et Biologiques pour la Santé (UTCBS), Faculté de Sciences Pharmaceutiques et Biologiques, Paris 75270, France*

https://doi.org/10.1021/acs.analchem.4c02932
Anal. Chem. XXXX, XXX, XXX−XXX

Aynur Naghizade − *Laboratoire de Spectrométrie de Masse des Interactions et des Systèmes (LSMIS), Université de Strasbourg, CNRS UMR7140, CMC, Strasbourg 67081, France*

Lola Alez-Martin − *Laboratoire de Spectrométrie de Masse des Interactions et des Systèmes (LSMIS), Université de Strasbourg, CNRS UMR7140, CMC, Strasbourg 67081, France*

Oscar Hernandez-Alba − *Laboratoire de Spectrométrie de Masse BioOrganique (LSMBO), Université de Strasbourg, CNRS UMR7178, IPHC, Strasbourg 67037, France; Infrastructure Nationale de Protéomique ProFI - FR2048, Strasbourg 67087, France;* orcid.org/0000-0001-5524-4983

Armand Leclerc − *Centre de Recherche Astrophysique de Lyon (CRAL), Université Lyon 1, CNRS, UMR5574, ENS de Lyon, Lyon 69007, France*

Sarah Cianferani − *Laboratoire de Spectrométrie de Masse BioOrganique (LSMBO), Université de Strasbourg, CNRS UMR7178, IPHC, Strasbourg 67037, France; Infrastructure Nationale de Protéomique ProFI - FR2048, Strasbourg 67087, France;* orcid.org/0000-0003-4013-4129

Rabah Gahoual − *Université Paris Cité CNRS, Inserm, Unité de Technologies Chimiques et Biologiques pour la Santé (UTCBS), Faculté de Sciences Pharmaceutiques et Biologiques, Paris 75270, France;* orcid.org/0000-0001-8459-3138

Yannis-Nicolas Francois − *Laboratoire de Spectrométrie de Masse des Interactions et des Systèmes (LSMIS), Université de Strasbourg, CNRS UMR7140, CMC, Strasbourg 67081, France;* orcid.org/0000-0002-8776-071X

Complete contact information is available at: https://pubs.acs.org/10.1021/acs.analchem.4c02932

Notes

The authors declare no competing financial interest.

■ ACKNOWLEDGMENTS

The authors would like to thank every person that contributed to the achievement of this article. This research work was supported by the Agence National de la Recherche as part of the project MethAmAbs (project no. ANR-19-CE29-0009) the CNRS, and the French Proteomic Infrastructure (ProFI; ANR-10-INBS-08-03). OHA acknowledges the "Agence Nationale de la Recherche" for funding his JCJC project "ConformAbs" (ANR-21-CE29-0009-01).

■ REFERENCES

(1) Kaplon, H.; Crescioli, S.; Chenoweth, A.; Visweswaraiah, J.; Reichert, J. M. *mAbs* **2023**, *15* (1), 2153410.
(2) Hansel, T. T.; Kropshofer, H.; Singer, T.; Mitchell, J. A.; George, A. J. T. *Nat. Rev. Drug Discovery* **2010**, *9* (4), 325−338.
(3) Gunn, G. R.; Sealey, D. C. F.; Jamali, F.; Meibohm, B.; Ghosh, S.; Shankar, G. *Clin. Exp. Immunol.* **2016**, *184* (2), 137−146.
(4) Real-Fernández, F.; Cimaz, R.; Rossi, G.; Simonini, G.; Giani, T.; Pagnini, I.; Papini, A. M.; Rovero, P. *Anal. Bioanal. Chem.* **2015**, *407* (24), 7477−7485.
(5) Liang, M.; Klakamp, S. L.; Funelas, C.; Lu, H.; Lam, B.; Herl, C.; Umble, A.; Drake, A. W.; Pak, M.; Ageyeva, N.; Pasumarthi, R.; Roskos, L. K. *Assay Drug Dev. Technol.* **2007**, *5* (5), 655−662.
(6) Bobrovnik, S. A. *J. Biochem. Biophys. Methods* **2003**, *57* (3), 213−236.
(7) Bobrovnik, S. A. *Ukr. Biokhim. Zh.* **2000**, *72* (3), 133−141.
(8) Stevens, F. *Mol. Immunol.* **1987**, *24* (10), 1055−1060.
(9) Joyce, A.; Shea, C.; You, Z.; Gorovits, B.; Lepsy, C. *AAPS J.* **2022**, *24* (6), 114.
(10) Hofbauer, C. J.; Whelan, S. F. J.; Hirschler, M.; Allacher, P.; Horling, F. M.; Lawo, J.-P.; Oldenburg, J.; Tiede, A.; Male, C.; Windyga, J.; Greinacher, A.; Knöbl, P. N.; Schrenk, G.; Koehn, J.; Scheiflinger, F.; Reipert, B. M. *Blood* **2015**, *125* (7), 1180−1188.
(11) Dai, S.; Schantz, A.; Clements-Egan, A.; Cannon, M.; Shankar, G. *AAPS J.* **2014**, *16* (3), 464−477.
(12) Rispens, T.; Hart, M. H.; Ooijevaar-de Heer, P.; van Leeuwen, A.; Vennegoor, A.; Killestein, J.; Wolbink, G.-J.; van der Kleij, D. *J. Pharm. Biomed. Anal.* **2013**, *85*, 179.
(13) Svitel, J.; Boukari, H.; Van Ryk, D.; Willson, R. C.; Schuck, P. *Biophys. J.* **2007**, *92* (5), 1742−1758.
(14) Wadhwa, M.; Knezevic, I.; Kang, H.-N.; Thorpe, R. *Biologicals* **2015**, *43* (5), 298−306.
(15) Beeg, M.; Nobili, A.; Orsini, B.; Rogai, F.; Gilardi, D.; Fiorino, G.; Danese, S.; Salmona, M.; Garattini, S.; Gobbi, M. *Sci. Rep.* **2019**, *9* (1), 2064.
(16) Gahoual, R.; Busnel, J.-M.; Beck, A.; François, Y. N.; Leize-Wagner, E. *Anal. Chem.* **2014**, *86* (18), 9074−9081.
(17) Bitoun, S.; Hässler, S.; Ternant, D.; Szely, N.; Gleizes, A.; Richez, C.; Soubrier, M.; Avouac, J.; Brocq, O.; Sellam, J.; De Vries, N.; Huizinga, T. W. J.; Jury, E. C.; Manson, J. J.; Mauri, C.; Matucci, A.; Hacein Bey Abina, S.; Mulleman, D.; Pallardy, M.; Broët, P.; Mariette, X.; Abirisk, C.; Berenbaum, F.; Dieudé, P.; Bertin, P.; Dougados, M.; Miceli, C.; Pedriger, A.; Marotte, H.; Cantagrel, A.; Vittecoq, O.; Lequere, T.; Saraux, A.; Flipo, R.-M.; Sibilia, J.; Gottenberg, J. E.; Combe, B.; Morel, J.; Wendling, D.; Verhoef, C.; Van Rijswijk, M.; Nurmohamed, M.; Vultaggio. *JAMA Netw. Open* **2023**, *6* (7), No. e2323098.
(18) Reinert, T.; Gahoual, R.; Mignet, N.; Kulus, A.; Allez, M.; Houzé, P.; François, Y. N. *Pharm. Biomed. Anal.* **2023**, *233*, 115446.
(19) Bobaly, B.; D'Atri, V.; Goyon, A.; Colas, O.; Beck, A.; Fekete, S.; Guillarme, D. *J. Chromatogr. B: Anal. Technol. Biomed. Life Sci.* **2017**, *1060*, 325−335.
(20) Cole, D.; Young, G.; Weigel, A.; Sebesta, A.; Kukura, P. *ACS Photonics* **2017**, *4* (2), 211−216.
(21) Liebel, M.; Hugall, J. T.; Van Hulst, N. F. *Nano Lett.* **2017**, *17* (2), 1277−1281.
(22) Foley, E. D. B.; Kushwah, M. S.; Young, G.; Kukura, P. *Nat. Methods* **2021**, *18* (10), 1247−1252.
(23) Wagner, C.; Fuchsberger, F. F.; Innthaler, B.; Lemmerer, M.; Birner-Gruenberger, R. *Int. J. Mol. Sci.* **2023**, *24* (13), 11033.
(24) Young, J. W.; Pfitzner, E.; Van Wee, R.; Kirschbaum, C.; Kukura, P.; Robinson, C. V. *iScience* **2024**, *27* (2), 108785.
(25) Olerinyova, A.; Sonn-Segev, A.; Gault, J.; Eichmann, C.; Schimpf, J.; Kopf, A. H.; Rudden, L. S. P.; Ashkinadze, D.; Bomba, R.; Frey, L.; Greenwald, J.; Degiacomi, M. T.; Steinhilper, R.; Killian, J. A.; Friedrich, T.; Riek, R.; Struwe, W. B.; Kukura, P. *Chem.* **2021**, *7* (1), 224−236.
(26) Den Boer, M. A.; Lai, S.-H.; Xue, X.; Van Kampen, M. D.; Bleijlevens, B.; Heck, A. J. R. *Anal. Chem.* **2022**, *94* (2), 892−900.
(27) Soltermann, F.; Foley, E. D. B.; Pagnoni, V.; Galpin, M.; Benesch, J. L. P.; Kukura, P.; Struwe, W. B. *Angew. Chem., Int. Ed.* **2020**, *59* (27), 10774−10779.
(28) Li, Y.; Struwe, W. B.; Kukura, P. *Nucleic Acids Res.* **2020**, *48* (17), No. e97.
(29) Reinert, T.; Houzé, P.; Francois, Y.-N.; Gahoual, R. *J. Chromatogr. B: Anal. Technol. Biomed. Life Sci.* **2024**, *1234*, 123974.
(30) Friguet, B.; Chaffotte, A. F.; Djavadi-Ohaniance, L.; Goldberg, M. E. *J. Immunol. Methods* **1985**, *77* (2), 305−319.
(31) Van Stappen, T.; Brouwers, E.; Tops, S.; Geukens, N.; Vermeire, S.; Declerck, P. J.; Gils, A. *Ther. Drug Monit.* **2015**, *37* (4), 479−485.
(32) Nelson, J. T.; Kim, S.; Reuel, N. F.; Salem, D. P.; Bisker, G.; Landry, M. P.; Kruss, S.; Barone, P. W.; Kwak, S.; Strano, M. S. *Anal. Chem.* **2015**, *87* (16), 8186−8193.
(33) Klasse, P. J. *Expert Rev. Vaccines* **2016**, *15* (3), 295−311.